Structural, electronic, and surface properties of anatase TiO_2 nanocrystals from first principles

Amilcare Iacomino,[1] Giovanni Cantele,[2] Domenico Ninno,[2] Ivan Marri,[3] and Stefano Ossicini[3]
[1]*Dipartimento di Fisica "E. Amaldi," Università degli Studi Roma Tre, Via della Vasca Navale 84, I-00146 Roma, Italy and CNISM, U. di R. Università degli Studi di Napoli Federico II, Dipartimento di Scienze Fisiche, Complesso Universitario Monte S. Angelo, Via Cintia, I-80126 Napoli, Italy*
[2]*CNR-INFM-Coherentia and Università degli Studi di Napoli Federico II, Dipartimento di Scienze Fisiche, Complesso Universitario Monte S. Angelo, Via Cintia, I-80126 Napoli, Italy*
[3]*CNR-INFM-S3 and Dipartimento di Scienze e Metodi dell'Ingegneria, Università di Modena e Reggio Emilia, Via Amendola 2 Pad. Morselli, I-42100 Reggio Emilia, Italy*
(Received 2 May 2008; published 5 August 2008)

The structural and electronic properties of anatase TiO_2 nanocrystals (NCs) are investigated through first-principles calculations. The dependence of the structural properties (e.g., NC volume variations) on the surface chemistry is discussed by considering two different surface coverages (dissociated water and hydrogens). Both prevent a pronounced reconstruction of the surface, thus ensuring a better crystalline organization of the atoms with respect to the bare NC. In particular, the results for the hydrated NC do show the largest overlap with the experimental findings. The band-gap blueshift with respect to the bulk shows up for both the bare and the hydrated NC, whereas hydrogen coverage or oxygen desorption from the bare NCs induce occupied electronic states below the conduction levels thus hindering the gap opening due to quantum confinement. These states are spatially localized in a restricted region and can be progressively annihilated by oxygen adsorption on undercoordinated surface titanium atoms. Formation energy calculations reveal that surface hydration leads to the most stable NC, in agreement with the experimental finding that the truncated bipyramidal morphology is typical of the moderate acidic environment. Oxygen desorption from the bare NC is unfavorable, thus highlighting the stabilizing role of surface oxygen stoichiometry for TiO_2. Available experimental data on the electronic and structural properties of TiO_2 NCs are summarized and compared with our results.

DOI: 10.1103/PhysRevB.78.075405 PACS number(s): 61.46.Hk, 71.15.Mb, 81.07.Ta

I. INTRODUCTION

The popularity of titanium dioxide (TiO_2) comes from its multifunctional properties making it one of the most investigated metal oxides. TiO_2, mainly employed in chemistry, is essentially a wide gap cheap biocompatible semiconductor with striking photocatalytic capabilities in several heterogeneous reactions. Applications in the field of electronic devices, polluting compounds decomposition, protection of artistic works from oxidation, medical bioengineering, photoreactions for specific syntheses, solar energy conversion with optimal quantum yields, and production of molecular hydrogen from water is driven through years to a widespread scientific literature.[1] The list of TiO_2 applications is still growing since the advent of nanotechnology, with peculiar properties of this promising material emerging at the nanoscale.[2,3]

TiO_2 nanocrystals (NCs) are mostly synthesized with sol-gel methods showing a high degree of crystallinity.[4] Crystal phase and morphology are strongly affected by synthesis conditions, however both theoretical and experimental results proved the anatase polymorph to be favored for the smallest samples (<14 nm) and for the acidic pH to stabilize truncated tetragonal bipyramidal NCs with [101], [011], [010], and [001] facets.[5–9] The aim of this study is to give an insight into the structural and electronic properties of TiO_2 NCs with differently covered surfaces, using *ab initio* density-functional theory (DFT) calculations. Following the suggestions proposed by Polleux *et al.*,[9] we consider truncated bipyramidal systems, with [101] and [011] as lateral surfaces and [001] as the truncation surface, to model the experimentally observed nanostructures. An analogous morphology was recently proposed by Wu *et al.*[10] as preferable for dye-sensitized solar cells. The request of smallness of the systems due: to computational effort, to stoichiometry to avoid problems of charging, to the highest coordination for each atom to support their formal oxidation state (i.e., O^{2-} and Ti^{4+}) were not an easy task to be simultaneously fulfilled, as previously reported by Persson *et al.*[11] Moreover the pure (or bare) anatase NC presented in this work are somehow connected with the NC studied in a recent work of Barnard *et al.*[12] At the end we retained bipyramids with truncation along the [001] direction thus eliminating most of the undercoordinated atoms whose number raises coming closer to the NC tip. This choice meets the experimental evidence that bipyramids are always truncated or smoothed at the tips due to growing dynamics, surface tension, and functionalizing adsorbates.[8,9] Indeed our choice is also suitable for aligning and assembling NCs in longer chains since tipped bipyramids would produce too narrow necks. There are many open questions about nanostructured TiO_2, some of which are object of this work and are summarized in the following:

For structural properties the reduction in sample size produces an unavoidable variation of the structural arrangement. Lattice parameters have been observed to expand in some cases[13] or to contract in others,[14] while rutile and other metal oxides show a linear expansion by decreasing the particle size. A dependence on the preparation method is also observed: sol-gel/hydrolysis methods lead to lattice strain, expansion, and Ti deficiency, whereas nonhydrolytic sol-gel

routes lead to pure and stoichiometric samples with nonlinear volume contraction.[13]

In the bulk anatase, a titanium (Ti) atom is in the center of an octahedron whose vertices are occupied by six oxygens (O). This coordination is preserved in internal NC cells but the surface truncation produces undercoordination, dangling bonds, and surface tension whose effect is a local disorder.[15] Some experimental works had observed the variation of bond lengths and coordination numbers upon decreasing the NC size, in the smallest samples (<5 nm).[15–19] This suggests an influence of the surface on the overall structure. Reactive compounds in solution can change the NC morphology as proved by the restoring of the octahedral coordination for the surface Ti atoms after adsorption of radicals.[16,20]

For electronic properties the anatase TiO_2 crystal is an indirect semiconductor with an energy gap of 3.2 eV.[1] On a theoretical general ground, a decrease in the dimensions down to the nanometer scale makes the electron mean-free path comparable to system size; thus, one would expect a quantum size (Q-size) effect to be measurable through the band-gap blueshift. This shift is not always detectable in nanostructured TiO_2: (i) some authors[4,21,22] observed the bulk gap for sample diameters down to 1.5 nm; (ii) others[2,23,24] measured a blueshift already in the range 5–10 nm (just recently, a clear detection of the blueshift for both anatase and rutile polymorphs has been observed[25]); (iii) a redshift is also observed and is mainly ascribed to the presence of surface oxygen vacancies[26,27] (behaving as shallow traps for photogenerated charge carriers), to adsorbates, or to dopants producing electronic states in the forbidden region.[2] The nature of the first allowed transition is still under debate as well since a direct radiative decay blueshift of the band gap is advised.[3,21,28]

For surface functionalization TiO_2 is the best candidate for photovoltaic solar cell conversion of light with water splitting and consequent hydrogen production on a large scale.[1,29] This ambitious goal needs a deep understanding of the interaction of TiO_2 with water and its constituents. The presence of a large hydration sphere surrounding TiO_2 nanoparticles is usually detected,[30] for example by infrared spectrum analysis,[31] and may play a fundamental role in photocatalysis. This hydration sphere is built up of different and nonequivalent bonds between water and the TiO_2 surface[32] and of weak hydrogen bonds among water molecules[31] (thus forming a multilayered wet sphere[30]). The first water coverage can be made up of both a dissociative and a molecular chemisorption[33] on the NC surface but the dissociative adsorption seems to be favored,[34] being capable to fill possible oxygen vacancies in the synthesis process. Early works directly focused on the TiO_2-H surface interaction and doping of NCs have been reported very recently.[35,36] Keeping this in mind we decided to cover our bare systems with simple adsorbates (H_2 and H_2O), modeling simple and stable surface configurations in presence of hydrogens and hydration.

It is evident that the very numerous experimental data on TiO_2 NCs produced a large variety of, often conflicting, results. The lack of a satisfactory and organic comprehension of many of the measured properties can certainly be ascribed to the TiO_2 own nature—very high reactivity toward the external environment, ability to sustain complex surface chemistry, O vacancies, etc. The aim of this work is to shed light, at least partially, on some of these aspects. First-principles calculations based on DFT will be applied to NCs with different surface coverages. Structural and electronic properties will be analyzed and compared with experiments.

In Sec. II we summarize the method and computational details and we define the NCs studied in this work. In Sec. III A we discuss the results on the NC reconstruction in presence of different surface coverages. In Sec. III B we study the NC electronic properties. The nature of the electronic levels is elucidated from density-of-states (DOS) calculations and from plots of the highest occupied and lowest unoccupied molecular orbitals (HOMO and LUMO, respectively). In Sec. III C we discuss the formation energy of the NCs. We will show that the hydrated NC is the most stable, whereas the hydrogen covered NC (representative of an extreme acidic condition) is the most unstable one.

II. METHODOLOGY

All first-principles calculations are carried out within the DFT framework, employing the QUANTUM-ESPRESSO package[37] based on plane waves and pseudopotentials. We used the generalized gradient approximation (GGA) parametrized with the Perdew-Wang (PW91) exchange-correlation functional[38] and Vanderbilt ultrasoft pseudopotentials.[39] The reciprocal space is sampled using a plane-wave basis set with a kinetic-energy cutoff of 30 Ry for the wave functions. The NC geometries are optimized with the direct energy minimization technique of Broyden-Fletcher-Goldfarb-Shanno,[40] which is a quasi-Newton method based on the construction of an approximated Hessian matrix at each system relaxation step. The optimization is stopped when each Cartesian component of the force acting on each atom is less than 0.026 eV/Å and the total energy difference between consecutive steps is less than 10^{-4} eV. All properties presented in the next sections are referred to the optimized systems. A vacuum gap of at least 6 Å separates each NC from its periodic replica in neighbor supercells to avoid spurious interactions. The convergence of the geometry, the electronic properties, the formation, and total energy with respect to the above parameters has been carefully checked.

The structural optimization of the tetragonal three-dimensional anatase crystal gives the lattice constants $a=3.809$ Å and $c=9.604$ Å, whereas the internal dimensionless parameter is $u=0.208$. All three numbers compare well with the experimental values (at 15 K) 3.782 Å, 9.502 Å, and 0.208, respectively.[41] The starting geometry of the bare TiO_2 NC is defined with atoms at the ideal crystal positions. The atomic positions were then randomized by 1% breaking symmetries and thus ensuring an unconstrained and more physical relaxation.

The bare stoichiometric NC (sc29) presented in this work is made up of 87 atoms with chemical formula $(TiO_2)_{29}$ (see Fig. 1). Its morphology derives from a perfect bipyramid with [101] and [011] lateral surfaces and is then truncated along [001], [100], and [010] directions. To ensure the stoichiometry four oxygen atoms—in the crystal

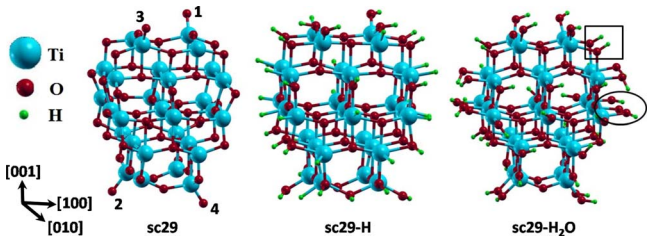

FIG. 1. (Color online) Optimized structures of the stoichiometric NCs presented in this work. The one-coordinated oxygens are labeled in the left NC in the same order as they are removed to form substoichiometric bare NCs nc29-*M*O (see text). In the hydrated NC (on the right) the box shows some chemisorbed OH groups labeled as OH^{in} in the text, whereas the circle shows some examples of chemisorbed OH groups labeled as OH^{out} in the text.

configuration—were added on the [001] surfaces labeled as one-coordinated oxygens (see Fig. 1). Several efforts to relax the system with these atoms placed on the square base of the structure did not converge, probably revealing the relevance of the TiO_2 anisotropy along the [001] direction.[1] The resultant morphology is not easy to explain since it can be viewed as an ellipsoid or a quasisphere anyhow nanofaceted, resembling the model obtained by Dzwigaj *et al.*[42] on a study of hydrated anatase surfaces. For the two different surface coverages that we propose each Ti atom is coordinated at least with four oxygens and each O atom is coordinated at least with two titanium atoms except the four one-coordinated oxygens.

The first surface coverage of sc29 is achieved by bonding each undercoordinated surface atom with one hydrogen (H) atom at a distance of 1 and 1.75 Å from an oxygen and a titanium atom, respectively.[43] The resulting NC (sc29-H), with chemical formula $(TiO_2)_{29}H_{48}$, can model the NC in extreme acidic environments but cannot attempt to restore an octahedral coordination of surface Ti atoms[44] (see Fig. 1). It can also model the exposure of dehydrated NCs to a H_2 atmosphere.[36]

The second surface coverage is obtained from sc29-H by replacing hydrogens bonded to surface Ti atoms with OH groups, which we label as OH^{out}. On the other hand, we label the bridging surface oxygens bonded to adsorbed H as OH^{in} (see Fig. 1) since this difference will be useful in the following. One more OH group is added to each of the four Ti atoms in the square base vertices to close their octahedral coordination.[45] The final NC (sc29-H_2O) has the chemical formula $(TiO_2)_{29}(H_2O)_{24}$ (see Fig. 1). This coverage can model the NC in a moderate acidic environment where OH groups account for the presence of functionalizing moieties, which stabilize the NCs through their radicals, or be viewed as a complete dissociative adsorption of water in the first layer of the hydration sphere. Hence this covered NC is among the simplest (and also stablest) models of the first layer of the hydration sphere.

At last, we studied the desorption of single oxygen atoms from sc29. We eliminated one at a time the four one-coordinated oxygens bonded on the surface of the optimized sc29. The resulting structures will be referred to as nc29-*M*O, with $M=\{1,2,3,4\}$. These surface bonds are considered important reactive sites in the nanocrystalline TiO_2 activity.[46]

For all the above described NCs we also computed the ionization potential (*IP*) and the electron affinity (*EA*) defined as $IP=[E(N-1)-E(N)]$ and $EA=[E(N)-E(N+1)]$, respectively. Here $E(N)$ represents the total energy of the neutral NC, whereas $E(N+1)$ $[E(N-1)]$ represents that of the negatively (positively) charged NC. A rigid shift has been applied to all the computed DOS, in such a way that $E_{HOMO}=-IP$ for each NC (E_{HOMO} being the HOMO energy).

III. RESULTS AND DISCUSSION

In the next sections we will systematically draw a parallelism between our findings and available experimental data.

A. Structural properties

1. NCs volume

The volume expansion or contraction of each NC has been evaluated by comparing the volume of the optimized NC with that of the NC, with the atoms at the bulk positions. The volume of a given NC is computed as $V=\Delta x\Delta y\Delta z$ (Δi is the dimension along the $i=\{x,y,z\}$ axis, computed as the distance between the two outermost Ti atoms along that direction).

From Table I it can be seen that only sc29 has an appreciable volume contraction (−11.5%) whereas sc29-H and sc29-H_2O are slightly expanded (less than 5%). Since both trends are actually observed,[13,14] it was argued a dependence on the composition and preparation conditions[13] (for example, Li *et al.*[14] attributed the contraction to a positive pressure of hydration sphere). Our results show that the contrac-

TABLE I. Dimensions (Δx, Δy, Δz), volume ($V=\Delta x\Delta y\Delta z$), and volume variations [$\Delta V=(V-V_0)/V_0$, with V_0 being the volume of the NC with the atoms in the ideal bulk positions] of the stoichiometric and passivated NCs. Δx, Δy, and Δz are calculated as distances along the respective axes between two outermost Ti atoms.

System	Δx (Å)	Δy (Å)	Δz (Å)	V (Å^3)	ΔV (%)
Bulk	7.618	7.618	9.604	557.36	
sc29	7.253	7.261	9.361	492.99	−11.5
sc29-H	7.755	7.945	9.247	569.74	+2.2
sc29-H_2O	7.815	7.728	9.604	579.79	+4.0

TABLE II. Experimental ranges of variation (Refs. 15–19 and 49) of Ti-O distances (Ti fixed, O up to the fifth coordination shell), Ti-Ti distances (third and fourth coordination shell), and coordination number (CN) in TiO_2 NCs. In parentheses the respective experimental values for the bulk are shown for comparison.

Shell	Atoms	Distance (Å)	CN
1st	Ti-O	1.95–1.72(1.93)	5.8–2.8(4)
2nd	Ti-O	2.01–1.99(1.98)	4.0–2.1(2)
3rd	Ti-Ti	3.13–3.02(3.04)	3.3–1.5(4)
4th	Ti-Ti	3.88–3.78(3.78)	3.0–0.7(4)
5th	Ti-O	3.88–3.77(3.87)	5.0–4.0(8)

tion is more likely a property of the bare NCs since the two coverages induce the opposite effect (as, for example, observed by Swamy *et al.*[13]).

By analyzing the variations along the three crystallographic axes, we find the contraction of the bare sc29 in each direction more pronounced in the basal plane (−4.8%) than along the z axis (−2.5%). This overall contraction was also experimentally reported by Choi *et al.*[47] Passivated NCs show an expansion in the basal plane (1.4%–4.3%) whereas, along z, sc29-H contracts (−3.7%) and sc29-H_2O keeps unchanged, thus revealing another effect of the anisotropy of the [001] direction. This behavior is also reported by Swamy *et al.*,[13] who experimentally observed an expansion of the lattice constant a and the decrease in c. Swamy attributed the small expansion to a Ti deficiency. Our results show that particular surface configurations may contribute to determine this tendency. An expansion of anatase nanoparticles in water was also reported in a molecular dynamics study of Erdin *et al.*,[48] showing that anatase NCs preferentially expand in the basal plane.

2. Bond lengths in the octahedron and distances of atomic pairs

To investigate the local order and the surface reconstruction of our optimized systems, bond length and distance distribution are analyzed. As a reference, we report in Table II the ranges of variation of distances and coordination numbers (CN) deduced from all available experimental works[15–19,49] (the samples in these works are prepared with sol-gel methods and with diameters ranging from 1.9 to 20 nm and nearly spherical in shapes).

In Fig. 2 we report the Ti-O and Ti-Ti distance distribution. A dispersion around ideal bulk values (dotted vertical lines) is found as expected for strongly confined NCs due to local disorder and reconstruction. However, while for sc29-H and mostly sc29-H_2O, the peaks corresponding to the bulk distances are clearly distinguishable for sc29 the distance distribution shows many more peaks. We conclude that the surface coverage stabilizes a better crystalline organization with respect to the bare NC. Experimentally, a decrease in the CN and a broadened distribution of their values are observed (see Table II). The peaks 1^a, 1^b, and 1^c of Fig. 2 reveal that the Ti-O first shell tends toward contraction in all of the NCs, in agreement with experimental findings.[15,16]

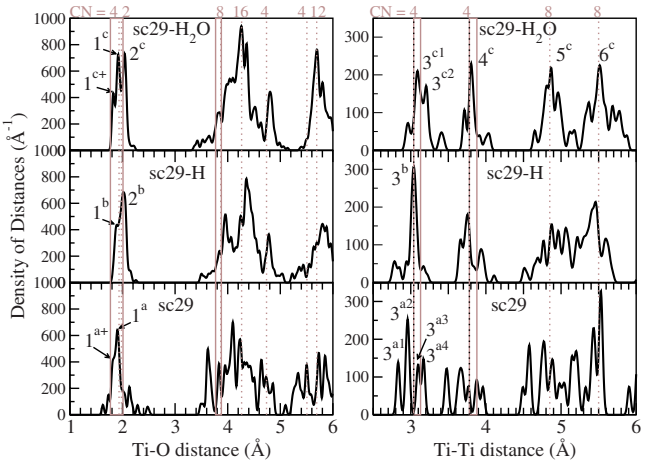

FIG. 2. (Color online) Calculated density distribution of Ti-O (left panel) and Ti-Ti (right panel) distances. Dotted vertical lines correspond to bulk distances (with the respective CN on the top). Experimental results lie within the vertical (gray) lines. The numbered peaks are described in the text. A fictitious Gaussian broadening (σ=0.03 Å) is attributed to each distance to give an easier picture and each curve is normalized to the total number of distances.

This is more evident for sc29, for which most of the distances are less than 1.93 Å and the second shell does not show up as a sharp peak. In sc29-H the decrease in the Ti-O first shell bond length is less pronounced and it is contrasted by an increase of bonds in the range of the second shell (peak 2^b). The decrease in the first shell length in sc29-H_2O is as well contained (peak 1^c) except for an amount of bonds shaping the peak 1^{c+} at the shortest distances.

Experimental samples show a reconstructed octahedron with three short and three long bonds,[18,19] whereas for the bulk anatase four short and two long bonds are found (4:2 ratio). To address this point we considered as Ti-O first shell all the bonds shorter than 1.95 Å (average of the first and the second shell length), hence the longer bonds are considered as Ti-O second shell. We find that the bare sc29 is closest to the bulk ratio with 2.23 (sc29-H is unbalanced to 0.56), whereas sc29-H_2O is the closest to experimental samples with 1.05.

Higher Ti-O shells are not experimentally analyzed since it is difficult to fit diffraction patterns for small NCs. However, sc29 shows a general trend of CN decreasing and distance contraction (larger disorder), whereas sc29-H and (to a larger extent) sc29-H_2O main peaks are close to the bulk values (thus ensuring a better structural organization, see Fig. 2).

In the Ti-Ti third shell variation, longer distances[15,17] and a decreased CN with respect to the bulk distance are experimentally observed.[18,19,47] The bare sc29 shows a pronounced decrease of CN (see Fig. 2, peaks $3^{a1}-3^{a4}$). The hydrogenated sc29-H is the closest to the bulklike behavior with a single well defined peak (3^b) at the bulk value. The hydrated sc29-H_2O has two main peaks (3^{c1} and 3^{c2}) at longer distances than the bulk value, which do not cause an excessive decrease in the CN, thus reproducing both experimental findings.

The observed Ti-Ti fourth shell slight expansion[17] is best reproduced by sc29-H_2O with its main peak (4^c). Higher Ti-Ti shells are broadened but hydration keeps distances at the bulk values better than the other surface configurations (see Fig. 2, peaks 5^c and 6^c).

In conclusion, the water coverage (representative of moderate acidic environment) is the best model for real NCs since it is capable to intercept all experimental findings, whereas full hydrogen coverage (representative of extreme acidic environment) shows an overestimation of experimental trends. The overall trend for the bare NC is toward contraction and to a more disordered reconstruction. Moreover the two simple surface coverages proposed in this work as models of two configurations of the hydration sphere are able to preserve a bulk structure of the NCs better than their bare counterpart. This conclusion is in agreement with the results of a molecular dynamics study by Koparde *et al.*[50]

Finally, to explain the two main experimental findings (i.e., the decrease in the first shell Ti-O bond and the equality of the first and second shell CN), the contributions of different atomic pairs to the peaks of Fig. 2 can be separated out. From this analysis on sc29-H_2O, we find that: (i) bulk oxygens (threefold coordinated) faithfully reproduce the 2:1 ratio of the distances in the bulk octahedron, thus other oxygens are the source of experimental variations; (ii) the increase in the second shell CN is entirely caused by surface (H-bonded) oxygens; and (iii) oxygens coming from covering hydroxyl groups determine the first peak at 1.83 Å (peak 1^{c+}). We thus find that OH^{out} radicals, adsorbed on the surface of NCs, are the main source of the first shell contraction actually observed.[15,16] On the other hand, the experimental evidence of the 1:1 ratio of the first two shells[18,19] can be entirely ascribed to chemisorption of OH^{in} groups (see Fig. 1). Thus we can clearly link the two main experimental variations to two different sources that is the adsorption of two kinds of OH groups on the NC surface. At last, isolated and then highly reactive oxygen—possibly present on the NC surface—may produce the shortest bonds [<1.79 Å (Ref. 16)] as shown for sc29.

As a final remark, we point out that the adsorption of hydrogen gives rise to bonds with a very narrow distribution (with a 0.03 Å range). The sc29-H shows a mean Ti-H distance of 1.72 Å, slightly smaller than the initial value of 1.75 Å. The O-H bond mean value is 0.98 Å for all NCs (slightly reduced with respect to the initial value of 1.00 Å), in agreement with the result of Erdin *et al.*[48]

B. Electronic properties

In this section we discuss the electronic properties of the NCs by analyzing the DOS, the DOS projected (PDOS) on the atomic orbitals and charge-density plots.

1. From crystal to NC

First of all, we compare the electronic properties of the bare sc29 NC with those of the bulk. The electronic levels span four energy ranges, well separated by energy gaps [panels (a)–(d) in Fig. 3].

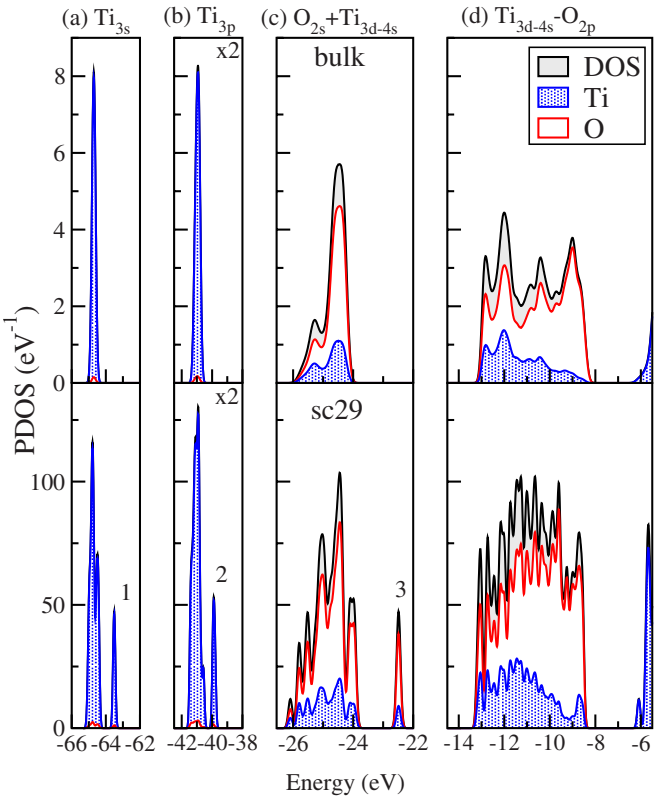

FIG. 3. (Color online) DOS and PDOS for bulk anatase TiO_2 (top panels) and the sc29 NC (bottom panels). The peaks labeled 1–3 are discussed in the text. The four occupied groups of levels and their respective atomic character are labeled on the top. The alignment has been performed by shifting the HOMO level of the cluster to the calculated value of the ionization potential. For graphical purposes the bulk DOS is shifted so as the top valence band matches the sc29 HOMO energy. DOS and PDOS curves are calculated by assigning a Gaussian broadening of 0.1 eV to each Kohn-Sham energy level.

The first [Fig. 3(a)] and second [Fig. 3(b)] groups of levels have a very dominant Ti 3*s* and Ti 3*p* atomic character, respectively, thus they can be considered semicore states that do not take part significantly to the chemical bond with oxygen atoms. For sc29 these two groups of levels span an energy range of 0.60 and 0.88 eV, respectively, larger than the respective range in the crystal (higher panels in Fig. 3, 0.07 and 0.65 eV, respectively). This apparently contradicts an expected narrowing due to the quantum confinement. Actually, this occurrence can still be attributed to the reduced size, enhancing the role of the surface. This can be inferred from the detached peaks at higher energy present in the first three groups of levels of the NC (see bottom panels of Fig. 3, peaks 1, 2, and 3). Peaks 1 and 2 belong to the titania bonded to the four one-coordinated oxygens on the surface, while peak 3 is due to those oxygens. Peak 2 can be connected to the results recently obtained by Thomas *et al.*[51] on resonant photoemission measurements of the Ti 3*p* electronic states of the anatase [101], [001], and rutile [110] surfaces. In that case, the Ti 3*p* related states have a tail at lower binding energy than the bulk peak. The tail is ascribed to the outermost Ti^{3+} atoms of oxygen deficient or defective surfaces. In

our case they are related to the interaction of Ti atoms with one-coordinated surface oxygens, for which a double bond nature is suggested.[16] The desorption of these oxygens (nc29-*M*O NCs, see Fig. 1) leads to the progressive approaching of the peak to the bulk peak and an increasing number of occupied Ti 3*d* states, whose nature will be discussed later.

The third group of states has a dominant O 2*s* atomic character and shows hybridization with the Ti_{4s-3d} atomic orbitals. Its width is even, in this case, larger for the NC (2.14 eV) than for the crystal (1.47 eV).

The last occupied group has the hybrid Ti_{4s}-O_{2p} and Ti_{3d}-O_{2p} characters. In this case the group widths are similar, 4.50 eV for the crystal and 4.63 eV for sc29, and can be compared with the experimental value for bulk anatase of 4.70 eV.[52]

The *Q*-size effect is better shown in the last two groups by the presence of narrower and sharper peaks in the DOS and most of all by the widening of the band gap. The anatase crystal is an indirect semiconductor with the first transition ($M \rightarrow \Gamma$) at 3.2 eV. Our calculation on the anatase crystal gives a gap of 2.13 eV, which well compares with other theoretical works based on the DFT,[53] but it is clearly an underestimation of the real band gap (this is an usual shortcoming of DFT). The HOMO-LUMO gap in the NC is 2.46 eV showing a blueshift of 0.33 eV. The first group of empty states has a dominant Ti 3*d* character at the onset with an increasing O 2*p* hybridization character for both systems. From this first analysis we deduce that, in the range of 1 nm, two different and likely competing effects showed up. The *Q*-size effect is present due to the reduced size but the spreading of the states all over the system makes them influenced by the surface structure. The overall behavior of the electronic states is thus the result of the two effects.

2. *Effects of the surface coverage*

The main difference introduced by the surface coverages in the two semicore groups of levels is the absence of the detached peaks observed in sc29. They are ascribed to the Ti atoms bonded with the one-coordinated oxygens on the [001] surfaces (see bottom panels of Fig. 4, peaks 1, 2, and 3). These oxygens are H-bonded for both coverages, thus becoming twofold coordinated.

The third group of levels [see Fig. 4(c), dominant atomic character O 2*s*] is strongly affected by the surface bonds. For both coverages, the levels mainly related to H-bonded oxygens (group of peaks A and C) are all located at higher binding energies than those related to unsaturated oxygens (group of peaks B and D). At variance, in sc29, the levels related to undercoordinated surface oxygens (the H-bonded ones in sc29-H) are all located at lower binding energies. Thus the surface coverage induces a level shift of these O 2*s* orbitals to higher binding energies than those related to bulklike oxygens.

The most interesting changes concern the higher-energy valence levels [see Fig. 4(d)], as explained in the following:

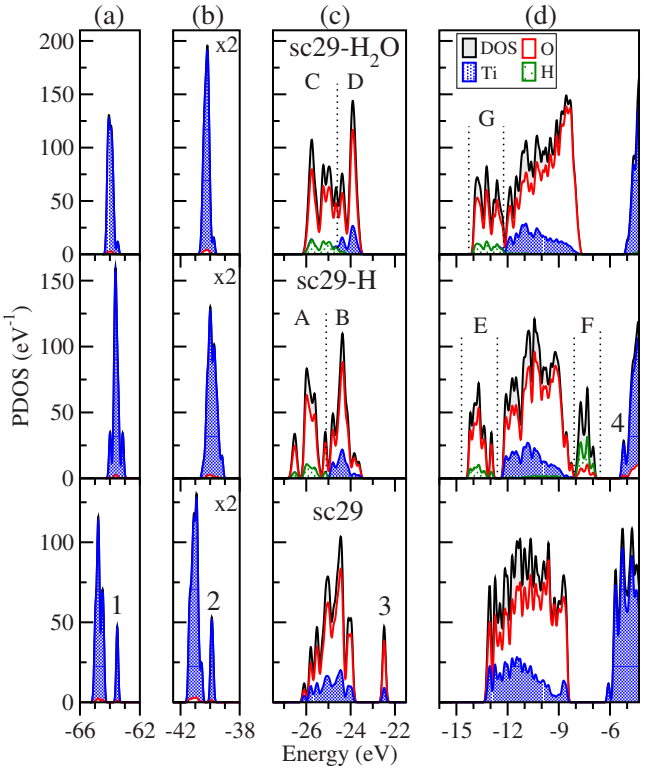

FIG. 4. (Color online) DOS and PDOS for sc29 (bottom panels), sc29-H (middle panels), and sc29-H_2O (top panels). The four groups of occupied levels are labeled on the top, panels (a) to (d). The numbered peaks (1, 2, 3, and 4) are discussed in text. Vertical dotted lines highlight the groups of levels (A–G) discussed in the text. A rigid shift has been applied to the DOS of all the NCs to bring the HOMO energy to the value of the computed ionization potential.

For O-H bonds both sc29-H and sc29-H_2O do show, in this energy range, a subgroup of levels with higher binding energies than those related to the (bulklike) Ti-O bonds. Such subgroups are labeled E and G and are ascribed to the O_{2p}-H_{1s} chemical bond. From a deeper analysis of the subgroup G in sc29-H_2O, it turns out that the higher binding energy levels are due to O-H bonds within chemisorbed OH^{in}, whereas the lower binding energy levels are due to chemisorbed OH^{out} radicals. Thus, it is possible to distinguish the effect of the two types of chemisorbed OH radicals in stabilizing the electronic levels, as it happens for the structural reconstruction of the octahedron (see Sec. III A).

For Ti-H bonds hydrogen coverage produces an occupied subgroup of states in the forbidden bulk gap [labeled F in Fig. 4(d)], just above the (bulklike) Ti-O valence-band (VB) states, whereas the hydrated sc29-H_2O results in a significant increase in the DOS below the (surface) O 2*p* HOMO energy. The subgroup F is substantially related to the Ti_{3d-4s}-H_{1s} chemical bond, absent in the bare and hydrated NCs. Therefore, the reduction of Ti atoms promoted by the formation of Ti-H bonds leads to the opposite effect with respect to the Ti-OH bond: occupied states show up at lower binding energy than the typical top valence states of TiO_2 (antibonding O 2*p* derived bands). This effect can be a source of a possible redshift of the band gap, eventually hid-

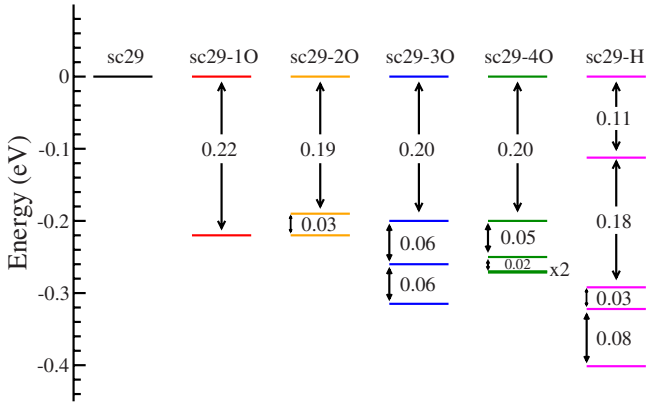

FIG. 5. (Color online) Scheme of the intragap energy levels of the hydrogenated and O deficient NCs. All LUMO energies are placed to 0 eV for graphical purposes. The HOMO-3 level of sc29–4O is double degenerate, as indicated by the label.

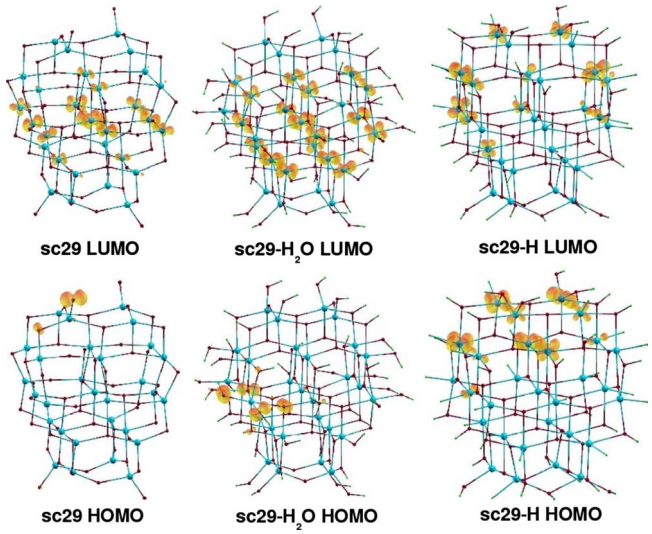

FIG. 6. (Color online) Charge-density contour plots of the HOMOs and LUMOs states of stoichiometric NCs. The contours correspond to 10% of the maximum value.

ing the blueshift caused by the Q-size effect. The very presence of these subgap states shows that the hydrogen coverage does not provide an ideal hydrogen passivation of the system.[54] The gap between the top (barelike) occupied level and the onset of the subgroup F is 0.35 eV. Similar intragap states have been actually observed and ascribed to the hydration sphere, whose Ti-OH and Ti-H_2O bonds have induced occupied states above the VB of about 0.6 and 0.54 eV, respectively.[55] On the contrary, our results show that Ti-OH bonds do not induce states in the gap but they stabilize states to higher binding energies than the VB. The intragap states do depend from possible Ti-H bonds, which can be formed on the surface of the NCs (for example, due to the steric hindrance of the same hydration sphere).

3. Band gap

The blueshift obtained for the bare NC (0.25 eV) is enhanced in sc29-H_2O, showing a forbidden gap of 2.83 eV (i.e., a blueshift of 0.70 eV). We expect that the Q-size effect can be detectable in stoichiometric TiO_2 NCs and, mostly, it can be preserved by some configurations of the hydration sphere. In fact, the experimentally observed blueshift is sometimes ascribed to direct allowed transitions[21,23] in an otherwise indirect semiconductor. However our results show that even the direct transition is blueshifted. Of course the small exciton radius of TiO_2 ($R_{ex} \sim 1$ nm) (Ref. 21) makes it difficult to detect the Q-size effects since it requires the synthesis of very small NCs. Furthermore, such NCs may show properties strongly dependent on the structural relaxation, the crystal purity, and the surface properties. Our results are in agreement with the very recent experimental work of Satoh *et al.*,[25] who observed band-gap blueshifts in the range 0.22–0.69 eV for anatase NCs with diameters in the range 1.64–1.02 nm. These authors have also pointed out the importance of crystallinity on the Q-size effects, as they have detected different blueshifts ascribable to rutile and anatase NCs of comparable dimension. In our case, this dependence on the structural organization is linked to the surface coverage, as it is capable to preserve a better crystallinity (see Sec. III A). In fact the blueshift of the hydrated NC (0.70 eV) is closer to the experimental value (0.69 eV) with respect to the bare sc29 (0.33 eV).

In Fig. 5 we sketch some examples of the different phenomena, which do occur with other surface configurations. The hydrogen coverage of the bare NC leads to the presence of four occupied energetic levels near the conduction band (CB) [see Fig. 4(d), peak 5], which considerably reduce the gap to 0.11 eV. In the same way the progressive desorption of the one-coordinated oxygens from the [001] surface leads to NCs (nc29-MO, $M=\{1,2,3,4\}$) with an energy gap of about 0.2 eV and an increasing content of occupied states near the CB whose occupation number is always twice the number of desorbed oxygens.

4. HOMO-LUMO states

In this section we comment on the spatial distribution of the HOMO, LUMO, and the intragap states of the hydrogen covered sc29-H and substoichiometric nc29-MO NCs, respectively. The knowledge of these key features can help in understanding the photoactivity of TiO_2 NCs since the location of reactive sites and the pathways of charge transfer are originated by the overlap of the wave functions and by the energetic proximity among excitable and available single states.

HOMO and LUMO charge-density contour plots are depicted in Fig. 6. The sc29 HOMO originates from an O $2p$ orbital, which is also typical of the valence-band maxima of TiO_2 crystals.[52] It is a localized surface state and no hybridization with Ti orbitals occurs (see Fig. 6). Similarly, the sc29-H_2O HOMO is O $2p$ in character but its spatial distribution is affected by the degeneracy of the highest occupied energetic levels, as previously shown in Fig. 4. On the contrary, the sc29-H HOMO shows an exclusive Ti $3d$ character and its spatial distribution involves Ti atoms localized in a restricted region of the NC. In general, the Ti $3d$ orbital character of electronic states is due to free CB electrons,[52] to defect sites caused by oxygens deficient structures,[51] or to

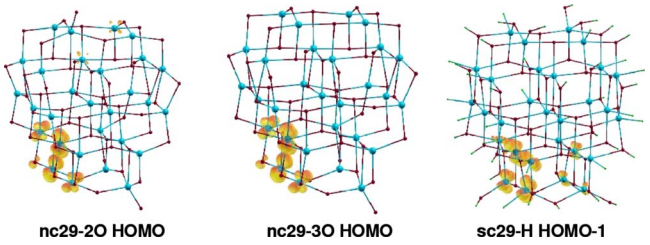

FIG. 7. (Color online) Charge-density contours plots of some occupied states of O deficient or hydrogenated NCs. The contours correspond to 10% of the maximum value.

photogenerated traps.[56,57] The oxygens vacancies can determine intragap occupied states immediately above the VB (Ref. 52) or below the CB edge.[58] In our case, the sc29-H HOMO is a defect state just below the conduction levels (HOMO-LUMO gap is 0.11 eV, see Fig. 5). It is worthwhile to note that this result can be linked to the very recently observed formation of Ti 3*d* occupied states, in the dark and at low temperatures, due to the hydrogen coverage of NCs.[35,36] The other three occupied states below this HOMO also have Ti 3*d* character and are localized in the region of one of the two [001] surfaces (see as example the HOMO-1 level in Fig. 7). It is interesting to note that the Ti atoms involved in these states are indifferently bonded to hydrogen or oxygen.

All the LUMOs have Ti 3*d* character, as expected for the TiO_2 conduction levels[52] but the spatial distribution of the sc29-H LUMO differs from the others, since it involves only the outermost titania (see Fig. 6 top right). The sc29 and sc29-H_2O LUMOs are delocalized in the bulk, showing Ti 3*d* levels spread either all over the structure (sc29-H_2O) or on a "bulk" plane of Ti atoms (sc29). On the contrary, sc29-LUMO is surface delocalized as for two-dimensionally delocalized shallow traps revealed by electron paramagnetic resonance (EPR) measurements.[58–60] This information can be particularly useful for the synthesis of TiO_2 nanofilms made up of NCs whose conductive properties are liked to be tuned.

Another result concerns the four defect states of sc29-H, namely, HOMO-3 to HOMO. We can infer that the reduction of the bare NC with hydrogens does not produce any charge transfer from the Ti 3*d* defect sites to the nearest hydroxylic groups if we consider these aspects: (i) the difference between sc29-H and sc29-H_2O is the substitution of the Ti-H bonds with Ti-OH ones; (ii) the defect sites are absent in the hydrated sc29-H_2O, thus unveiling the electron donor behavior of hydrogens in sc29-H; (iii) the defect sites involve titania of Ti-H as well as of Ti-OH bonds; and (iv) there is no hybridization of the defect sites in sc29-H with H 1*s* orbitals, on the contrary they show a pure Ti 3*d* character. This occurrence was reported by Henderson *et al.*[61] on measurements regarding the TiO_2 [110] surface where the charge transfers from the defective Ti 3*d* to the bonded hydroxylic group only. This result also confirms that surface Ti-OH species are unlikely to be electron donors as it has been recently reported.[35] This information can be useful to understand the electronic pathways in the photocatalytic activity of TiO_2 NCs.

The desorption of the four one-coordinated oxygens from the bare sc29 produces defect sites below the conduction levels. The number of such sites equals the number of desorbed oxygens (see Fig. 5). They are all Ti 3*d* in atomic character and are localized on the surface region surrounding the desorbed oxygens (see Fig. 7). The electron scavenging action of adsorbed oxygens involves, at first, deep defect sites and then shallow energy sites, thus narrowing and quenching the distribution of defect states below the CB. An analogous result is reported by de la Garza *et al.*,[62] who observed a progressive removal of surface sites of TiO_2 nanoparticles by increasing the concentration of dopamine, which restores the octahedral coordination of surface Ti atoms with its OH bidentate ligands.

TABLE III. Formation energy (E_f), passivation energy (E_p), formation energy per TiO_2 unit (E_f/N), and adsorption energy per passivating molecule (E_p/M). The values are obtained from Eq. (1) and Eq. (2), and are all expressed in eV.

System	E_f	E_f/N	E_p	E_p/M
sc29	−140.37	−4.84		
sc29-H	−130.02	−4.48	10.35	0.43
sc29-H_2O	−164.03	−5.66	−23.66	−0.99

C. Formation energies

The formation energy of a given NC is defined by

$$E_f = E_{\text{tot}} - M_x \cdot \mu_x - N \cdot \mu_{\text{TiO}_2}, \tag{1}$$

where E_{tot} is the total energy of the system, M_x is the number of covering molecules having chemical potential μ_x ($x=H_2$; H_2O), and N is the number of TiO_2 units (with chemical potential μ_{TiO_2}). The chemical potentials are chosen as the total energy of the correspondent isolated molecules.

The energy required to cover the surface with adsorbates, referred to as passivation energy with respect to the bare NC sc29, is defined by

$$E_p = E_{\text{tot}} - M_x \cdot \mu_x - E_{\text{tot}}^{\text{sc29}}, \tag{2}$$

where E_{tot} is the total energy of the covered system, $E_{\text{tot}}^{\text{sc29}}$ is the total energy of the bare sc29, and M is the total number of covering molecules. All data are shown in Table III.

All NCs have negative formation energies (column E_f). The highest E_f per TiO_2 molecule is −4.48 eV of sc29-H, while the lowest is −5.66 eV of sc29-H_2O (column E_f/N). The passivation energy with molecular hydrogens costs 0.43 eV per H_2 molecule, while dissociative adsorption of molecular water is −0.99 eV per H_2O molecule (column E_p/M).

The hydrated NC is the most stable and this is consistent with our initial assumption that truncated bipyramidal morphologies are characteristic of moderate acidic aqueous solutions. The stabilizing role of dissociative adsorption of water on the overall energetics of nanophase samples has

TABLE IV. Calculated EA and IP of all the TiO_2 NCs.

System	EA (eV)	IP (eV)
sc29	3.72	8.55
nc29–1O	3.52	6.39
nc29–2O	3.35	5.95
nc29–3O	3.17	5.78
nc29–4O	3.06	5.63
sc29-H	2.71	4.98
sc29-H_2O	2.83	7.82

been observed[34] and it has been also suggested by theoretical works.[48]

The desorption energy ΔE_O of an oxygen atom, one-coordinated on the surface of sc29, is calculated from

$$\Delta E_O = \left(E_M^{\text{tot}} + \frac{M}{2} \cdot \mu_{O_2} - E_{\text{sc29}}^{\text{tot}} \right) / M, \tag{3}$$

where $M=\{1,2,3,4\}$, E_M^{tot} is the total energy of nc29-MO, μ_{O_2} is the chemical potential of a spin polarized isolated oxygen molecule, and $E_{\text{sc29}}^{\text{out}}$ is the total energy of sc29. The result is 3.47 eV for each oxygen, which shows that the stoichiometric NC is the most stable, that these oxygens sites are independent, and lastly that the oxygen desorption from these NCs is unfavorable. It should be pointed out that the four oxygens are one coordinated to the surface Ti atoms, which became fourfold coordinated in this way, thus ensuring a better stabilization of undercoordinated titanium atoms with strong bonds.

Using the Makov-Payne correction for charged systems,[63] we calculated the electron affinity (EA) and the ionization potential (IP) of our NCs with results shown in Table IV. The sc29 ionization potential of 8.55 eV is in the range of values of 8.37–9.98 eV calculated by Qu and Kroes[64] for TiO_2 NCs composed by up to 15 molecular units, whereas its electron affinity of 3.72 eV is between the adiabatic and vertical detachment energy (3.6–4.80 eV) measured by Zhai and Wang[65] on an anionic $(TiO_2)_{10}$ NC. Progressive oxygen desorption from sc29 lowers more and more both the electron affinity and the ionization potential and can be rationalized as the effect of the presence of defective electronic states, near in energy to empty conductive states. This trend is confirmed by hydrogen covered sc29-H, which as well presents defective states. Hydrated sc29-H_2O shows a high ionization potential of 7.82 eV (which can be connected to that of sc29) but a low electron affinity of 2.83 eV (which is close to that of sc29-H).

IV. CONCLUSIONS

We performed DFT calculations on TiO_2 NCs with different surface coverages, modeling different synthesis conditions. From a thorough analysis of the experimental findings we identified the relevant ranges of variation of the main structural and electronic properties. The comparison with our calculations allowed us to interpret some controversial properties of TiO_2 NCs. The main properties that we highlighted are summarized in the following: (1) The bare stoichiometric NC undergoes a global structural contraction, whereas surface coverage induces volumetric expansion. The contraction of sc29 occurs in each direction, thus the same trend is expected for TiO_2 NCs not subjected to an external pressure. On the contrary, the interaction with adsorbates produces an expansion, which is more evident along the basal direction than on the [001] surfaces. This explains the observed expansion of the cell parameter a and the slight contraction of c. (2) All the NCs show the contraction of the first shell Ti-O bond length, but only hydration leads to a 1:1 ratio of the first and second shell coordination numbers (i.e., the observed rearrangement of the Ti-O bond lengths in the octahedron). Thus, from the hydrated NC, we link these two results to two surface bonds of different nature: (i) Ti-OH bonds, with the hydroxylic radical adsorbed *on* the undercoordinated Ti of the surface, lead to short Ti-O bonds; (ii) OH, adsorbed *in* the surface of NCs as bridging groups between Ti atoms, induce long Ti-O bonds. (3) The surface coverage prevents a pronounced reconstruction of the surface, thus leading to a more bulklike organization of the whole structure. In particular, the hydrated NC more closely reproduces the observed variations with respect to the bulk structural properties. (4) The small exciton radius of TiO_2 ($R_{ex} \sim 1$ nm) (Ref. 21) makes it difficult to observe the Q-size effects. Our NCs are thus well suited ($2R_{NC} \sim R_{ex}$) to detect such possible effects. In fact, the quantum confinement of the electronic states can be deduced from the tendency to discretization of the electronic levels and from the blueshift of the band gap. This shift and the shape of the DOS depend on the NC crystallinity since we showed that each surface coverage induces a different local and hence global spatial reconstruction. Such a result agrees with recent experimental observations.[25] However the decrease in the NC dimension down to the nanoscale enhances the surface role, as well. Hence, Q-size effects can be hidden in the presence of particular surface morphologies. For example, hydration stabilizes all the dangling bonds to higher binding energies than the valence states of the NC, whereas the chemical reduction of the same NC with hydrogen coverage induces intragap states. Furthermore, the surface configuration affects the energy distribution of the electronic states down to the semicore states. (5) Occupied electronic states in the range 0.11–0.40 eV below the conduction levels are induced by oxygen desorption and reduction with hydrogen of titanium atoms. These states are Ti $3d$ in atomic character and are spatially localized in restricted regions of the NCs. Adsorption of oxygen decreases the number of these states from the deepest energetic levels on, similarly to the effect induced by dopamine bidentate ligands on defect sites.[62] No complete charge transfer occurs from these defect sites to the hydroxylic groups, as experimentally observed for surfaces.[61] (6) At last, the hydration leads to the most stable NC. This is consistent with the experimental evidence that truncated bipyramidal NCs are characteristic of moderate acidic environments and that the first layer of water coverage on TiO_2 nanosamples is preferentially constituted of dissociated water. Oxygen adsorption is as well favored, since it restores the octahedral coordination of surface titanium atoms.

ACKNOWLEDGMENTS

We acknowledge the support of the MIUR PRIN Italy. All of the calculations were performed at CINECA-Bologna (Iniziativa Calcolo Parallelo del CNR-INFM) and "Campus Computational Grid" Università di Napoli Federico II. A.I. acknowledges CNISM for the financial support.

[1] U. Diebold, Surf. Sci. Rep. **48**, 53 (2003).
[2] O. Carp, C. L. Huisman, and A. Reller, Prog. Solid State Chem. **32**, 33 (2004).
[3] M. Fernández-García, A. Martínez-Arias, J. C. Hanson, and J. A. Rodriguez, Chem. Rev. (Washington, D.C.) **104**, 4063 (2004).
[4] M. Niederberger, M. H. Bart, and G. D. Stuchy, Chem. Mater. **14**, 4364 (2002).
[5] A. S. Barnard and L. A. Curtiss, Nano Lett. **5**, 1261 (2005).
[6] H. Zhang and J. F. Banfield, J. Phys. Chem. B **104**, 3481 (2000).
[7] Y. Gao and S. A. Elder, Mater. Lett. **44**, 228 (2000).
[8] C. H. Cho, M. H. Han, D. H. Kim, and D. K. Kim, Mater. Chem. Phys. **92**, 104 (2005).
[9] J. Polleux, N. Pinna, M. Antonietti, C. Hess, U. Wild, R. Schlögl, and M. Niederberger, Chem.-Eur. J. **11**, 3541 (2005).
[10] J. Wu, S. Hao, J. Lin, M. Huang, Y. Huang, Z. Lan, and P. Li, Cryst. Growth Des. **8**, 247 (2008).
[11] P. Persson, J. C. M. Gebhardt, and S. Lunell, J. Phys. Chem. B **107**, 3336 (2003).
[12] A. S. Barnard, S. Erdin, Y. Lin, P. Zapol, and J. W. Halley, Phys. Rev. B **73**, 205405 (2006).
[13] V. Swamy, D. Menzies, B. C. Muddle, A. Kuznetsov, L. S. Dubrovinsky, Q. Dai, and V. Dmitriev, Appl. Phys. Lett. **88**, 243103 (2006).
[14] G. Li, L. Li, J. Boerio-Goates, and B. F. Woodfield, J. Am. Chem. Soc. **127**, 8659 (2005).
[15] L. X. Chen, T. Rajh, Z. Wang, and M. C. Thurnauer, J. Phys. Chem. B **101**, 10688 (1997).
[16] L. X. Chen, Tijana Rajh, W. Jäger, J. Nedeljkovic, and M. C. Thurnauer, J. Synchrotron Radiat. **6**, 445 (1999).
[17] V. Luca, S. Djajanti, and R. F. Howe, J. Phys. Chem. B **102**, 10650 (1998).
[18] K. L. Yeung, A. J. Maira, J. Stolz, E. Hung, N. K. Ho, A. C. Wei, J. Soria, K. Chao, and P. L. Yue, J. Phys. Chem. B **106**, 4608 (2002).
[19] K. L. Yeung, S. T. Yau, A. J. Maira, J. M. Coronado, J. Soria, and P. L. Yue, J. Catal. **219**, 107 (2003).
[20] T. Rajh, L. X. Chen, K. Lukas, T. Liu, M. C. Thurnauer, and D. M. Tiede, J. Phys. Chem. B **106**, 10543 (2002).
[21] N. Serpone, D. Lawless, and R. Khairutdinov, J. Phys. Chem. **99**, 16646 (1995).
[22] S. Monticone, R. Tufeu, A. V. Kanaev, E. Scolan, and C. Sanchez, Appl. Surf. Sci. **162-163**, 565 (2000).
[23] K. Madhusudan Reddy, S. V. Manorama, and A. R. Reddy, Mater. Chem. Phys. **78**, 239 (2003).
[24] L. Zhao and J. Yu, J. Colloid Interface Sci. **304**, 84 (2006).
[25] N. Satoh, T. Nakashima, K. Kamiruka, and K. Yamamoto, Nature (London) **3**, 106 (2008).
[26] W. F. Zhang, M. S. Zhang, Z. Yin, and Q. Chen, Appl. Phys. B: Lasers Opt. **70**, 261 (2000).
[27] I. Nakamura, N. Negishi, S. Kutsuna, T. Ihara, S. Sugihara, and K. Takeuchi, J. Mol. Catal. A: Chem. **161**, 205 (2000).
[28] T. Toyoda and I. Tsuboya, Rev. Sci. Instrum. **74**, 782 (2003).
[29] M. Ni, M. K. H. Leung, D. Y. C. Leung, and K. Sumathy, Renewable Sustainable Energy Rev. **11**, 401 (2007).
[30] J. Soria, J. Sanz, I. Sobrados, J. M. Coronado, A. J. Maira, M. D. Hernández-Alonso, and F. Fresno, J. Phys. Chem. C **111**, 10590 (2007).
[31] T. Bezrodna, G. Puchkovska, V. Shymanovska, J. Baran, and H. Ratajczak, J. Mol. Struct. **700**, 175 (2004).
[32] T. Bezrodna, G. Puchkovska, V. Shimanovska, I. Chashechnikova, T. Khalyavka, and J. Baran, Appl. Surf. Sci. **214**, 222 (2003).
[33] D. A. Panayotov and J. T. Yates, Jr., Chem. Phys. Lett. **410**, 11 (2005).
[34] A. A. Levchenko, G. Li, J. Boerio-Goates, B. F. Woodfield, and A. Navrotsky, Chem. Mater. **18**, 6324 (2006).
[35] D. A. Panayotov and J. T. Yates, Jr., Chem. Phys. Lett. **436**, 204 (2007).
[36] T. Berger, O. Diwald, E. Knözinger, F. Napoli, M. Chiesa, and E. Giamello, Chem. Phys. **339**, 138 (2007).
[37] S. Baroni, A. Dal Corso, S. de Gironcoli, P. Giannozzi, C. Cavazzoni, G. Ballabio, S. Scandolo, G. Chiarotti, P. Focher, A. Pasquarello, K. Laasonen, A. Trave, R. Car, N. Marzari, and A. Kokalj, http://www.pwscf.org.
[38] J. P. Perdew and Y. Wang, Phys. Rev. B **45**, 13244 (1992).
[39] D. Vanderbilt, Phys. Rev. B **41**, 7892 (1990).
[40] A. Mordecai, *Nonlinear Programming: Analysis and Methods* (Dover, New York, 2003).
[41] J. K. Burdett, T. Hughbanks, G. J. Miller, J. W. Richardson, Jr., and J. V. Smith, J. Am. Chem. Soc. **109**, 12 (1987).
[42] S. Dzwigaj, C. Arrouvel, M. Breysse, C. Geantet, S. Inoue, H. Toulhoat, and P. Raybaud, J. Catal. **236**, 245 (2005).
[43] A. S. Barnard and P. Zapol, Phys. Rev. B **70**, 235403 (2004).
[44] The attempt to close the octahedron of 4-fold coordinated surface Ti atoms with two hydrogens (H) failed, as these H pairs tended to detach from the NC and go together during the relaxation process, thus we discarded this possibility.
[45] We also neglected hydrogens bonded to the twofold-coordinated bridging oxygens of [001] surfaces as to ensure the stoichiometry of hydration sphere.
[46] M. J. Lundqvist, M. Nilsing, P. Persson, and S. Lunell, Int. J. Quantum Chem. **106**, 3214 (2006).
[47] H. C. Choi, Y. M. Jung, and S. B. Kim, Vib. Spectrosc. **37**, 33 (2005).
[48] S. Erdin, You Lin, J. W. Halley, P. Zapol, P. Redfern, and L. Curtiss, J. Electroanal. Chem. **607**, 147 (2007).
[49] M. Fernández-García, X. Wang, C. Belver, J. C. Hanson, and J. A. Rodriguez, J. Phys. Chem. C **111**, 674 (2007).
[50] V. N. Koparde and P. T. Cummings, J. Phys. Chem. C **111**, 6920 (2007).
[51] A. G. Thomas, W. R. Flavell, A. K. Mallick, A. R. Kumarasinghe, D. Tsoutsou, N. Khan, C. Chatwin, S. Rayner, G. C.

Smith, R. L. Stockbauer, S. Warren, T. K. Johal, S. Patel, D. Holland, A. Taleb, and F. Wiame, Phys. Rev. B **75**, 035105 (2007).

[52] R. Sanjinés, H. Tang, H. Berger, F. Gozzo, G. Margaritondo, and F. Lévi, J. Appl. Phys. **75**, 2945 (1994).

[53] Ming-Yu Kuo, C.-L. Chen, C.-Y. Hua, H.-C. Yang, and P. Shen, J. Phys. Chem. B **109**, 8693 (2005).

[54] In bulk TiO_2, Ti is in the formal oxidation state 4+ and sixfold coordinate, resulting in a donation of 2/3 electrons per bond. In this way the hydrogen coverage is not a true passivation, as it results in the reduction of Ti instead of an ideally expected oxidation.

[55] B. S. Liu, X. He, Y. J. Zhao, and Q. N. Zhao, Spectrosc. Spectral Anal. (Beijing) **26**, 208 (2006).

[56] S. H. Szczepankiewicz, A. J. Colussi, and M. R. Hoffmann, J. Phys. Chem. B **104**, 9842 (2000).

[57] S. Leytner and J. T. Hupp, Chem. Phys. Lett. **330**, 231 (2000).

[58] T. Berger, M. Sterrer, O. Diwald, E. Knözinger, D. Panayotov, T. L. Thompson, and J. T. Yates, Jr., J. Phys. Chem. B **109**, 6061 (2005).

[59] S. H. Szczepankiewicz, J. A. Moss, and M. R. Hoffmann, J. Phys. Chem. B **106**, 7654 (2002).

[60] T. Yoshihara, R. Katoh, A. Furube, Y. Tamaki, M. Murai, K. Hara, S. Murata, H. Arakawa, and M. Tachiya, J. Phys. Chem. B **108**, 3817 (2004).

[61] M. A. Henderson, W. S. Epling, C. H. F. Peden, and C. L. Perkins, J. Phys. Chem. B **107**, 534 (2003).

[62] L. de la Garza, Z. V. Saponjic, N. M. Dimitrijevic, M. C. Thurnauer, and T. Rajh, J. Phys. Chem. B **110**, 680 (2006).

[63] G. Makov and M. C. Payne, Phys. Rev. B **51**, 4014 (1995).

[64] Z.-W. Qu and G.-J. Kroes, J. Phys. Chem. C **111**, 16808 (2007).

[65] H.-J. Zhai and L.-S. Wang, J. Am. Chem. Soc. **129**, 3022 (2007).